Physica A 564 (2021) 125500

Contents lists available at ScienceDirect

Physica A

journal homepage: www.elsevier.com/locate/physa

A random multiplicative model of Piéron's law and choice reaction times

José M. Medina [*,1], José A. Díaz [1]

Universidad de Granada, Facultad de Ciencias, Departamento de Óptica, Edificio Mecenas, 18071, Granada, Spain

ARTICLE INFO

Article history:
Received 4 May 2020
Received in revised form 24 September 2020
Available online 2 November 2020

Keywords:
Decision making
Mental chronometry
Stochastic latency mechanisms
Information entropy
Power-law scaling

ABSTRACT

We present a random multiplicative model with additive noise of human reaction/response times based on the power-law function, Piéron's law. We study the role of weak additive noise in two different scenarios: in the first case, the multiplicative model describes the differences between simple, and two-choice reaction times in Piéron's law. In the second case, we investigate how choice reaction times depend on the transfer of information in neurons. A transition is found at 0.5 bits due to weak additive noise. Reaction times follow an U-shaped function that lead to both anti-Hick's and Hick's effects. We discuss the implications of random multiplicative processes, and minimum transfer of information in decision making, and neural control.

1. Introduction

Advances in modern mental chronometry has attracted attention into the potential benefits of fluctuation phenomena, and delayed decision making in the mammalian brain [1–3]. A reference paradigm concerns the human reaction/response time (RT), and is usually defined as the time elapses from stimulus onset until a response is made (e.g., vocal, manual, saccadic, etc.) [1,2,4–6]. RTs are intrinsically stochastic, and involve fast decision making in a wide variety of everyday tasks (e.g., driving safety, sports and board games, etc.). In a simple RT paradigm, only one stimulus, and one response are possible whereas choice RTs involve selection from among alternatives by using multiple stimuli and responses [1,5,6]. At least two psychophysical laws have been investigated extensively in RTs: Piéron's law, and Hick's law. Piéron's law describes the hyperbolic decay of the mean RT, μ, as a function of the stimulus strength, S, (e.g., luminance, loudness intensity, odorant concentration, etc.) by a power-law function [1,7–9]:

$$\mu = \mu_0 + \alpha S^{-p}, \tag{1}$$

being μ_0, and α, the asymptotic limit or plateau reached at high S values, and a normalizing factor, respectively. The scaling exponent p is a non-integer value that indicates the steepness of the hyperbolic decay [1,9]. Piéron's law is a classical example of psychophysical scaling in perception and action, and holds true in all sensory modalities [1,7–12], in both simple and choice RTs [13,14], and in certain animal models [15–17].Deviations from Piéron's law can be found at very high S values and the mean RT could increase from the plateau by following an open U-shaped function [18–20].

In choice RT tasks, Hick's law describes the increase of μ with the logarithmic of the number of stimulus–response alternatives, or equivalently, the number of bits involved on a task [1,21,22]:

$$\mu = \phi + \gamma \mathbb{H}, \tag{2}$$

---

[*] Corresponding author.
E-mail address: jmedinaru@cofis.es (J.M. Medina).

[1] Both authors have contributed equally to this work.

https://doi.org/10.1016/j.physa.2020.125500

being ϕ, and γ the intercept, and the slope, respectively, and $\mathbb{H}$ is a logarithmic function which denotes an information-theoretic metric measured in bits (e.g., Shannon information) [21,22].

Hick's law is considered a benchmark effect in human–computer interactions, and has been verified over a large class of experiments [21,22], including in certain animal models [17,22,23]. The slope of Hick's law depends on the stimulus–response configuration as well as on individual practice [22]. Departures from Hick's law have been reported for more than 10 alternatives or 3 bits of information, and the mean RT increases exponentially [17,22,24]. Further, a reverse or anti-Hick's effect have found in saccadic eye movements, and RTs decrease as the number of alternatives increases [22,25–28]

A long standing issue concerns the unification of both psychophysical laws, and their functional relevance in decision making as well as in sensory-motor control. A few sequential-sampling models have derived the functional form of both Piéron's law and Hick's law simultaneously [17,29]. Caballero et al. have introduced a Bayesian approach with multiple channels for sequential sampling and decision making [29]. A different approach was presented by Reina et al. by using a nest-site selection model. The model was applied to a colony of honey bees for collective decision making [17]. In that stochastic accumulator models the RT is divided in at least two different stages: a decision, and a non-decision time [1,3,6,9]. The decision stage plays a central role, and is modeled by accumulating noisy evidence or response preparation from stimulus until a threshold criterion or boundary is reached [3,22]. The non-decision stage is considered a residual fixed additive time offset. The plateau μ_0 in Piéron's law is often identified with that non-decision time, and has been treated as a free parameter or simplified to zero [17,29–31].

However, that models have ignored the range of empirical values spanned by μ_0 in each sensory modality and in different experimental conditions [1,7–11,14,22,32,33]. An implicit assumption is that the non-decision time in μ_0 includes the rest of components such as the encoding time, and the motor latency [3,17,22,29,34], but this is without preserving any chronological order. Further, sequential-sampling models often link neural activity with RTs by associating spike rates with noisy stimulus information during stochastic accumulation [3,17,29,30,34,35].

In previous studies, Pins and Bonnet [14] have found that the scaling exponent p remains unchanged, and the plateau μ_0 was higher when comparing two-choice versus simple RTs regardless of the complexity of the task [14]. Although sequential-sampling models can mimic the shape of Piéron's law and Hick's law [17,29,30], it is not clear whether they can describe the effects found by Pins and Bonnet in two-choice RTs [14], and whether they are also able, on one hand, to unify both Hick's and anti-Hick's effects and, in the other hand, to predict testable changes in the asymptotic plateau μ_0.

In the present study, we address the question whether both Piéron's power-law function and, Hick's and anti-Hick's effects can be derived from a common generative mechanism by treating the RT as a random multiplicative process with additive noise. Multiplicative growth processes are one common way to generate power-law functions with a wide number of applications in physics, biology, finance, etc. [36–39]. In our approach, we focus on an information-theoretic framework that derives Piéron's law from an optimal decision process within sensory systems [40]. We pose that the transfer of information in neurons leads to an internal threshold criterion by power-law scaling and modulates a form of signal-dependent neural noise. Contrary to sequential-sampling models [17,29–31], we show that the asymptotic term μ_0 depends on both sensory and decisional factors. In previous works, we have demonstrated the functional role of random multiplicative processes to derive the shape of RT distributions and Zipf's law, the effect of Weber's law in RTs, deviations from Piéron's law at high S values and deviations from fluctuation scaling in human color vision [41–47].

Here, we report that differences between simple and two-choice reaction times in Piéron's law [14], arise from an increase in the transfer of information at the threshold leading to weak additive noise. We found a transition around 0.5 bits [44], and Piéron's law diverges under the presence of weak additive noise as well. This noise-induced transition leads to both Hick's and anti-Hick's effects. In comparison to sequential-sampling models, we also discuss that power-law behavior in Piéron's law is intimately linked with neural activity by a form of symmetry or scale invariance [39,48–50]. We also discuss a plausible basis for optimal decision making based on the minimum transfer of information in sensory systems [44,50,51].

2. Theory

2.1. A derivation of Piéron's law

For generic RT task, we define the growth of RT in the time axis as an irreversible process that arises from a cascade of local stages. This implies a hierarchical organization or chronological order in the RT that must be compatible with the principle of causality (i.e., every effect or event has a possible cause) [52]. For instance, a response selection cannot be before in time than the stimulus encoding because the act of encoding contributes to produce that response selection, etc. We will introduce below that irreversibility results from the formation of a noisy internal threshold, and thus, generating stochastic or random phenomena. Our approach should be understood as an asymptotic result providing a coarse-grained time description of behavioral activity.

We derive Piéron's law from first principles by using the information-entropy function proposed by Norwich [40,53]:

$$H = \frac{1}{2\ln 2}\ln\left(1+\frac{\beta S^p}{t}\right), \tag{3}$$

begin β a coefficient.

The value of H in Eq. (3) has dimensions of bits, and its derivation can be found elsewhere [40,53–55]. The H-function is a Boltzmann-type entropy function that evolves continuously over time. It is related with the internal uncertainty state of post-receptoral neurons about how sensory receptors process an external input signal of strength S. A high value of the H-function means a high uncertainty within the sensory system, and vice versa [40]. In this framework, sensory perception is not instantaneous but occurs during a finite period of time. The initial stage divides the H-function in two separate regimes or phases [40]. In the first phase the sensory system is in an internal stage of maximum uncertainty, and the H-function reaches a maximum value. In the second phase the sensory system removes that uncertainty, and the H-function decreases monotonically over time to complete certainty (i.e., a gain of information) [40,53]. The RT can be defined as the time needed to gather ΔH bits of information [40,53]:

$$\Delta H = H(S, t_0) - H(S, t) \geq 0, \tag{4}$$

being t_0 and t the encoding time, and the time to react, respectively, with $0 < t_0 < t$ [40,53]. Eq. (4) denotes an irreversible process, and defines an information threshold in decision making. Initially, the sensory system does not accumulate information over time. The time t_0 is the delay produced by an efficient encoder at maximum entropy, and sets the origin of information [40–42,53].

Introducing Eq. (3) into Eq. (4):

$$\Delta H = \frac{1}{2\ln 2}\left[\ln\left(1 + \frac{\beta S^p}{t_0}\right) - \ln\left(1 + \frac{\beta S^p}{t}\right)\right], \tag{5}$$

and solving Eq. (5) for the time t [40,53]:

$$t = \left[\frac{1}{t_0 \exp(2\ln 2\Delta H)} - \frac{1 - \exp(-2\ln 2\Delta H)}{\beta S^p}\right]^{-1}. \tag{6}$$

There are two different limits in Eq. (6) to be evaluated. Firstly, there is a lack of response in the sensory system, and t diverges when the stimulus strength S approaches to S_0, being S_0 a just-threshold internal reference value that depends on ΔH [40,41,53]:

$$\lim_{t\to\infty} \beta S^p \equiv \beta {S_0}^p = t_0\left[\exp(2\ln 2\Delta H) - 1\right]. \tag{7}$$

Secondly, the asymptotic term or plateau in Eq. (6) is reached at large S values [40,53]:

$$\lim_{S\to\infty} t \equiv \mu_0 = t_0 \exp(2\ln 2\Delta H). \tag{8}$$

Substituting Eq. (7), and (8) into Eq. (6) [40,41,43,47,53]:

$$\mu \equiv\ t = \mu_0\left[1 - \left(\frac{S_0}{S}\right)^p\right]^{-1}, \tag{9}$$

Eq. (9) is only valid when the mean RT, μ, takes finite values ($\forall S > S_0$). Then, Piéron's law Eq. (1) is obtained by taking the first two terms of a geometric series expansion in Eq. (9) [43,52]:

$$\mu = \mu_0 + \mu_0\left[\left(\frac{S_0}{S}\right)^p + \left(\frac{S_0}{S}\right)^{2p} + \cdots\right], \tag{10}$$

with $\alpha \equiv \mu_0 {S_0}^p$ [43,47].

The information-theoretic model of Piéron's law in Eqs. (7)–(10) implies a chronological order that cannot be violated: t_0 must precede μ_0, and both must precede μ, ($0 < t_0 < \mu_0 < \mu$) [41–45,47]. Further, the asymptotic term μ_0 is not fixed but stochastic, and contains those initial stages related with the encoding time t_0 and the formation of the sensory threshold S_0 as show in Eqs. (7)–(8) [41]:

2.2. A random multiplicative approach to reaction times

A random multiplicative process can be defined by using a discrete time Langevin-type dynamics [56,57] as follows [41, 43–45]:

$$x_{n+1} = a_n x_n + b_n, \tag{11}$$

being x_{n+1} and x_n the RT at the stages n+1 and n, respectively. The subscript n refers to the time step and x_n precedes x_{n+1}. The coefficients a_n and b_n denote the multiplicative and the additive noise terms, respectively [47]. The additive term b_n is usually considered as a repelling barrier or repulsion from the origin and avoids that x_{n+1} drifts to zero when the multiplicative factor a_n shrinks to zero [39,56,58,59].

It is assumed that both multiplicative and additive noise are delta correlated with variance, $\langle a_i, a_j\rangle \propto D_a\delta_{ij}$ and $\langle b_i, b_j\rangle \propto D_b\delta_{ij}$, where D_a and D_b are the diffusion coefficients, indicating the average strength of interactions, and the bracket $\langle\cdots\rangle$ means time averaging over many trials or repetitions of the same experiment [47].

In our approach, we set $\langle a_n x_n\rangle \cong \langle a_n\rangle x_0$, being x_0 a reference time that will be clarified later [47]. The diffusion coefficients D_a and D_b are not fixed but stimulus-dependent [47]. The time average of both multiplicative and additive noise is set proportional to the variance by fluctuation scaling [60], and $\langle a_n\rangle \propto D_a \neq 0$, $\langle b_n\rangle \propto D_b \neq 0$ [41–43,47], and thus:

$$\mu \equiv t \equiv \langle x_{n+1}\rangle \cong D_a x_0 + D_b, \tag{12}$$

We associate Piéron's law as a special case of the generic stochastic Eq. (12) by rewriting the diffusion coefficients D_a, D_b, and the reference time x_0, in terms of the plateau μ_0, the coefficient α, and the scaling exponent p [47]. Here we consider the full approach of Piéron's law in Eq. (9) because it describes better the curvature effects of RTs at near-threshold conditions [41,42,44,45,47]. The diffusion coefficient of the multiplicative noise term D_a, and the reference time x_0 in Eq. (12) are related with the stimulus strength S, and the encoding time t_0, respectively in Eq. (9) [43,44]:

$$x_0 = t_0 > 0, \tag{13}$$

$$D_a = \left[1 - \left(\frac{S_0}{S}\right)^p\right]^{-1}. \tag{14}$$

By using the plateau μ_0 in Eq. (8), Eq. (12) becomes:

$$\mu = \exp(2\ln 2\Delta H) D_a t_0 \tag{15}$$

To examine the additive noise term in D_b, we use Eq. (7) to replace ΔH as a function of the sensory threshold $\beta {S_0}^p$. Eq. (15) can be written as follows:

$$\mu = \left(1 + \frac{\beta {S_0}^p}{t_0}\right) D_a t_0 = D_a t_0 + \delta {S_0}^p, \tag{16}$$

being $\beta = \delta/D_a$, and δ a normalizing coefficient. The additive noise term in Eq. (12) is related to the formation of the sensory threshold, $D_b = \delta {S_0}^p$. Here $\delta {S_0}^p$ acts as a repelling barrier from the origin located at the encoding time t_0. Therefore, the mean RT, μ, in Piéron's law drifts to that barrier at marked supra-threshold conditions, $\forall S \gg S_0 \Rightarrow D_a \rightarrow 1$, and from Eq. (16), $\mu \rightarrow t_0 + \delta {S_0}^p$.

To investigate the effects of the additive noise in Eq. (16) we define the following ratio [47,57]:

$$\rho = \sqrt{\frac{D_b}{D_a}} = \sqrt{\beta {S_0}^p} = \sqrt{\delta {S_0}^p}\sqrt{1 - \left(\frac{S_0}{S}\right)^p}. \tag{17}$$

Eq. (17) cannot be examined without further assumptions about the nature of the coefficient δ or the encoding time t_0 in Eq. (7). We have introduced in [47] an approach that consists in varying the stimulus strength S in the multiplicative diffusion coefficient from near- to supra-threshold conditions. Here we use a similar procedure by setting the contribution of the additive noise term as a fixed reference value, $\rho_0 = \sqrt{\delta {S_0}^p}$. Eq. (17) can be renormalized as follows:

$$\frac{\rho}{\rho_0} = \sqrt{1 - \left(\frac{S_0}{S}\right)^p}. \tag{18}$$

At marked supra-threshold conditions, Eq. (18) tends to unity, i.e., the additive noise prevails in Piéron's law ($\forall S \gg S_0 \Rightarrow \rho \rightarrow \rho_0$). However, at near-threshold conditions Eq. (18) tends to zero, i.e., the effects of the additive noise are diluted, and the multiplicative noise mainly modulates Piéron's law ($\forall S \sim S_0 \Rightarrow \rho \rightarrow 0$).

2.3. An interpretation of the scaling exponent p of Piéron's law

From Eq. (7), we set $\beta' {S_0}^p = \exp(2\ln 2\Delta H) - 1$, being $\beta' = \beta/t_0$, and for the transfer of information ΔH:

$$\Delta H = \frac{1}{2\ln 2}\ln\left(1 + \beta' {S_0}^p\right). \tag{19}$$

Eq. (19) maps the transfer of information, ΔH, into threshold-based units by using a logarithmic transformation of a power-law function. For low values of the normalized sensory threshold $\left(\beta' {S_0}^p \ll 1\right)$, Eq. (19) just indicates a power-law dependency, $\Delta H/\Delta H_0 \cong \beta' {S_0}^p$, being $\Delta H_0 = 1 / 2\ln 2$, a reference value. The scaling exponent p is the slope of that power-law relationship as expressed in log–log units; $\ln(\Delta H/\Delta H_0) \cong p \ln\left(\beta' S_0\right)$, and can be interpreted as an efficiency index related to the number of bits transmitted per sensory threshold.

3. Simulation results

3.1. The asymptotic term of Piéron's law

Fig. 1(a) represents ΔH as a function of the sensory threshold $\beta' S_0$ (in normalized units) for different values of the scaling exponent p of Piéron's law. There are two different regimes in Eq. (19). For a fixed threshold value lower than unity,

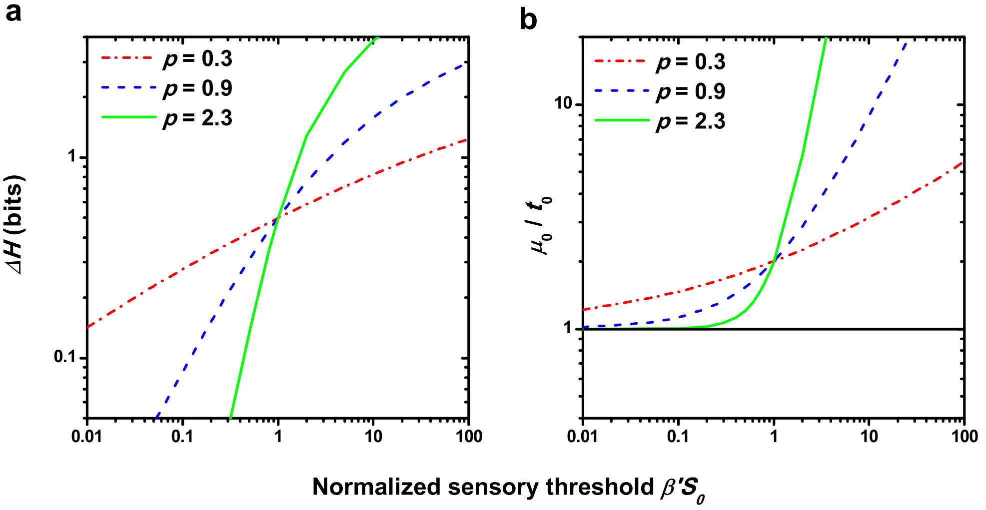

Fig. 1. Panels (a–b) double logarithmic plot of the transfer of information ΔH, and the plateau μ_0 (in normalized or t_0 units) of Piéron's law as a function of the sensory threshold $\beta' S_0$ (in dimensionless units). Solid, dashed and dash-dotted lines indicate different values of scaling exponent p.

$\left(\beta' S_0 < 1\right)$, the lower the value of p, $(0 < p < 1)$, the higher the transfer of information ΔH in neurons (e.g., simulated by $p < 1$, dashed and dash-dotted lines in Fig. 1(a)). However, an inverse tendency is found for threshold values higher than unity $\left(\beta' S_0 > 1\right)$, and ΔH is attenuated as the magnitude of the exponent p decreases. A transition is found at $\Delta H = 0.5$ bits $\left(\beta' {S_0}^p = 1\right)$. This issue will be further discussed below.

The minimum RT in decision making is giving by the plateau μ_0 of Piéron's law, and depends on the information transfer ΔH or equivalently, on the sensory threshold S_0. Introducing Eq. (19) into Eq. (8), $\mu_0 = t_0\left(1 + \beta' {S_0}^p\right)$. Fig. 1(b) represents the asymptotic term μ_0, normalized by the encoding time t_0, as a function of the normalized sensory threshold under the same simulation conditions as in Fig. 1(a). The plateau μ_0 increases as $\beta' S_0$ increases by means of a truncated power law function. Low values of the scaling exponent p enhances the rise of μ_0 for low values of the sensory threshold $\left(\beta' S_0 < 1\right)$ (e.g., simulated by $p < 1$, dashed and dash-dotted lines in Fig. 1(b)). After the transition at $\beta' {S_0}^p > 1$, that effect of the exponent p is reversed. The lower of value of $p < 1$, the smaller the plateau μ_0.

In general, ΔH in Eqs. (7), and (19), affects both S_0, and p, simultaneously. In the following sections, we have simplified the analysis of the additive noise in Piéron's law in two different scenarios. In the first case, ΔH mainly modulates S_0 and the scaling exponent p does not undergo abrupt changes over time [41,42,44,45]. In the second case, ΔH has a direct impact in p, and S_0, is approximately constant over time.

3.2. Piéron's law in simple and two-choice reaction times

In Eq. (9), we set the ratio $(S_0/S) = \left(\beta' S_0 / \beta' S\right)$, being $\beta' S$ the relative stimulus strength, $\beta' S \epsilon [0, \infty]$. By using Eq. (7), the full approach to Piéron's law in Eq. (9) can be rewritten as follows:

$$\frac{\mu}{t_0} = \exp(2 \ln 2 \Delta H) \left\{ 1 - \left[\frac{\exp(2 \ln 2 \Delta H) - 1}{\beta' S^p} \right] \right\}^{-1}, \tag{20}$$

and for the ratio ρ in Eq. (18):

$$\frac{\rho}{\rho_0} = \sqrt{1 - \frac{\exp(2 \ln 2 \Delta H) - 1}{\beta' S^p}}\,. \tag{21}$$

Fig. 2(a) represents the hyperbolic decay of the normalized RT μ as a function of the relative stimulus strength $\beta' S$, for different values of the transfer of information ΔH. The scaling exponent p was kept to a fixed value. The simulations capture the effects found by Pins and Bonnet in two-choice RTs [14].

Simple RTs imply the simplest task and are shorter. In our model, they correspond to those values that promote a lower transfer of information in decision making (e.g., simulated by $\Delta H = 0.35$ bits, solid line in Fig. 2(a)) or equivalently, a lower sensory threshold $\beta' S_0$ in accordance with Eqs. (7) and (19). However, Piéron's law in two alternative choice tasks are a direct consequence of higher ΔH values due to the problem difficulty (e.g., simulated by $\Delta H > 0.35$ bits, dashed, and dash-dotted lines in Fig. 2(a)), and the RT curves run in parallel to higher values to the right-up part. At marked supra-threshold conditions $(S \gg S_0)$, the asymptotic plateau is reached, and μ_0 increases as ΔH or $\beta' S_0$ increases, and thus, replicating the effect found by Pins and Bonnet [14].

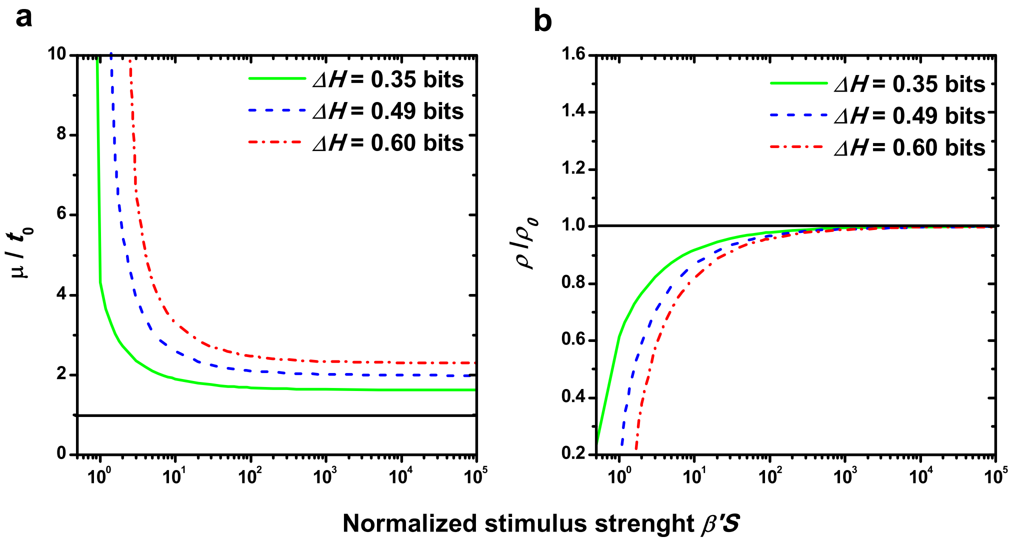

Fig. 2. Panels (a–b) show the semi-logarithmic plot of the mean RT μ (in normalized or t_0 units), and the ratio ρ/ρ_0 of the additive to multiplicative noise strength as a function of the relative stimulus strength $\beta'S$ (in normalized units), respectively. Solid, dashed, and dash-dotted lines indicate different values of the transfer of information ΔH. In all the examples, the scaling exponent of Piéron's law has a fixed value of $p = 0.6$. In both panels horizontal black solid lines indicate a ratio equal to unity.

Fig. 2(b) represents the ratio ρ/ρ_0 in Eq. (21) by using the same simulation parameters as in Fig. 2(a). In all cases, ρ increases as a function of the stimulus strength S, being the additive noise weaker near the threshold ($\rho \ll 1$). In two-choice RTs, additive noise is less persistent ($\rho \to 0$), and shifts to higher stimulus strength values up to $\beta'S = 10$ ($\Delta H > 0.35$ bits, dashed, and dash-dotted lines in Fig. 2(b)). After that regime, the multiplicative noise is no longer dominant at supra-threshold conditions, and the effect of the additive noise emerges by converging into a common value independently of ΔH $(\rho \to \rho_0)$.

3.3. *Piéron's law and the Hick's effect*

From Eq. (8), at very high S values, μ tends to the asymptotic plateau μ_0, and the RT shows an exponential increase as a function of ΔH [17,44]:

$$\lim_{S\to\infty} \mu = t_0 \exp(2\ln 2\Delta H). \tag{22}$$

The Hick's effect in Eq. (2) is obtained by taking the first two terms of a Taylor's series expansion in Eq. (22):

$$\mu = t_0 + (2\ln 2t_0)\,\Delta H + O\left(\Delta H^2\right) + \cdots, \tag{23}$$

being the intercept and the slope in Eq. (2), $\phi = t_0$ and $\gamma = 2\ln 2t_0$, and for the entropy function, $\mathbb{H} = \Delta H$.

It is important to bear in mind that the temporal evolution of the H-function in Eq. (4) is neither examined by using a probabilistic description of the number of stimulus–response alternatives nor treated as Shannon information entropy [17,21,22,29]. Thus, it cannot be compared directly with previous information-theoretic approaches to Hick's law [40]. Here, the higher the number of alternatives, the higher the transfer of information, ΔH, and the sensory system spends more time gathering information. Equivalently, by using Eq. (19), the sensory threshold $\left(\beta' S_0\right)$ increases and is more difficult to produce a voluntary RT due to the problem difficulty.

Fig. 3(a) represents the growth of Piéron's law in Eq. (20) as a function of ΔH, for different values of the relative stimulus strength $\beta'S$. The scaling exponent p remains fixed. At marked supra-threshold conditions, the effect of exponential growth in Eq. (22) shifts to the right to higher values of ΔH, and thus, extending the validity of the linear approximation given by the Hick's effect (e.g., simulated by $\beta'S > 500$, dashed and dash-dotted lines in Fig. 3(a)).

The effects of additive noise are shown in Fig. 3(b) for the same simulation conditions as in Fig. 3(a). The ratio ρ/ρ_0 decreases as ΔH increases and the effect of additive noise are diluted ($\rho \ll 1$) for $\Delta H > 2$ bits. However, that additive noise becomes more sustained at marked supra-threshold conditions ($\rho \to 1$) (e.g., simulated by $\beta'S > 500$, dashed and dash-dotted lines in Fig. 3(b)).

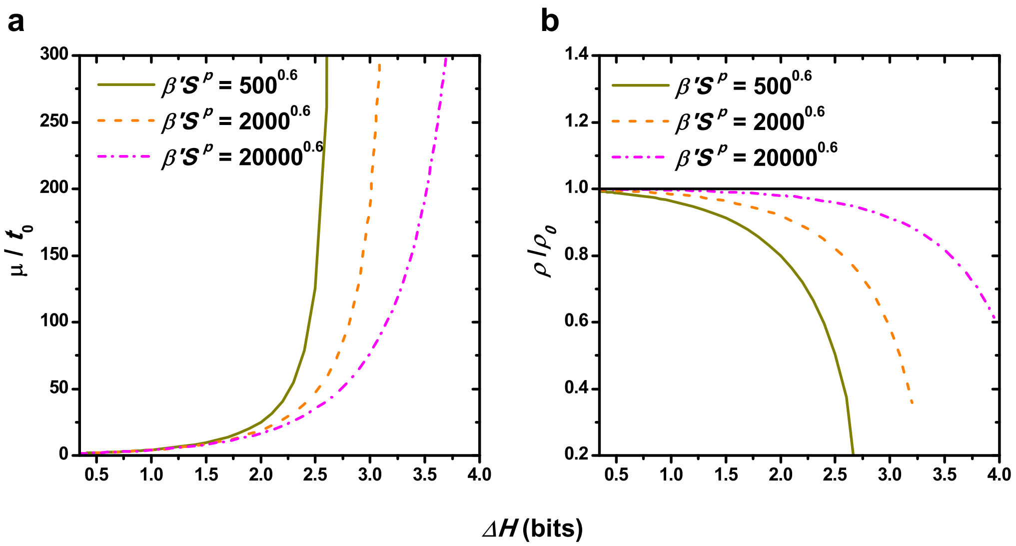

Fig. 3. Panels (a–b) show the mean RT μ (in normalized units), and the ratio ρ/ρ_0 of the additive to multiplicative noise strength as a function of the transfer of information ΔH. Solid, dashed, and dash-dotted lines indicate different values of the relative stimulus strength $\beta'S$. In all cases, the scaling exponent of Piéron's law has a fixed value of $p = 0.6$. In panel (b) the horizontal black solid line indicates a ratio equal to unity.

3.4. Piéron's law and the anti-Hick's effect

In this scenario, ΔH mainly modules the scaling exponent p and the sensory threshold $\beta' S_0{}^p$ remains fixed. From Eq. (19):

$$p = \frac{\ln\left[\exp\left(2\ln 2\Delta H\right) - 1\right]}{\ln\left(\beta' S_0\right)}. \tag{24}$$

Introducing Eq. (24) into Eq. (20):

$$\frac{\mu}{t_0} = \exp(2\ln 2\Delta H)\left\{1 - \left[\frac{\exp(2\ln 2\Delta H) - 1}{\beta' S^{\frac{\ln[\exp(2\ln 2\Delta H)-1]}{\ln(\beta' S_0)}}}\right]\right\}^{-1}, \tag{25}$$

and for the normalized ratio ρ in Eq. (18):

$$\frac{\rho}{\rho_0} = \sqrt{1 - \frac{\exp(2\ln 2\Delta H) - 1}{\beta' S^{\frac{\ln[\exp(2\ln 2\Delta H)-1]}{\ln(\beta' S_0)}}}}. \tag{26}$$

There is a singularity at $\Delta H = 0.5$ bits and the scaling exponent p in Eq. (24) equals to zero. In that situation, Piéron's law in Eq. (25) diverges and the ratio ρ in Eq. (26) equals to zero (i.e., a pure multiplicative process). That transition at $\Delta H = 0.5$ bits leads to two separate regimes: the first one includes those values below $\Delta H < 0.5$ bits and the second one, $\Delta H > 0.5$ bits.

Fig. 4(a) represents Piéron's law restricted to $\Delta H < 0.5$ bits for different values of the relative stimulus strength $\beta'S$. In this regime, the mean RT, μ, increases exponentially, and corroborates the Hick's effect at $\Delta H \ll 0.5$ bits, similar to Fig. 3(a). Higher values of $\beta'S$ enhance the multiplicative growth of RTs (e.g., simulated by $\beta'S > 1.5$, dashed and dash-dotted lines in Fig. 4(a)). The analysis of the normalized ratio ρ shows that the effects of the additive noise are weaker ($\rho \to 0$) near the transition zone, $0.45 \le \Delta H \le 0.49$ bits. Contrary to the tendency found in Fig. 3(b), here, the additive noise effects is more sustained for low values of the stimulus strength (e.g., simulated by $\beta'S = 1.5$, solid line in Fig. 4(b)).

Fig. 4(c) represents Piéron's law in the second regime after the transition, $\Delta H > 0.5$ bits. For high values of the relative stimulus strength $\beta'S$, the mean RT μ increases monotonically as in the previous Hick's effect. This is mainly due to the numerator at the right-hand side of Eq. (25), $\exp 2\ln 2\Delta H$, and the denominator does not contribute and approaches to unity (e.g., simulated by $\beta'S = 10$, dash-dotted line in Fig. 4(c)). However, at low values of the normalized stimulus strength $\beta'S$, an U-shaped function is clearly manifested. Within the interval, $0.51 \le \Delta H \le 1.2$ bits, the RT decreases as ΔH increases and thus, confirming the existence of an anti-Hick's effect in Piéron's law (e.g., simulated by $\beta'S < 10$, dashed and solid lines in Fig. 4(c)). Fig. 4(d) represents the normalized ratio ρ in the same simulation conditions as in Fig. 4(c). In comparison with Fig. 4(b), the ratio ρ shows an inverted trend and increases as ΔH increases up to the unity.

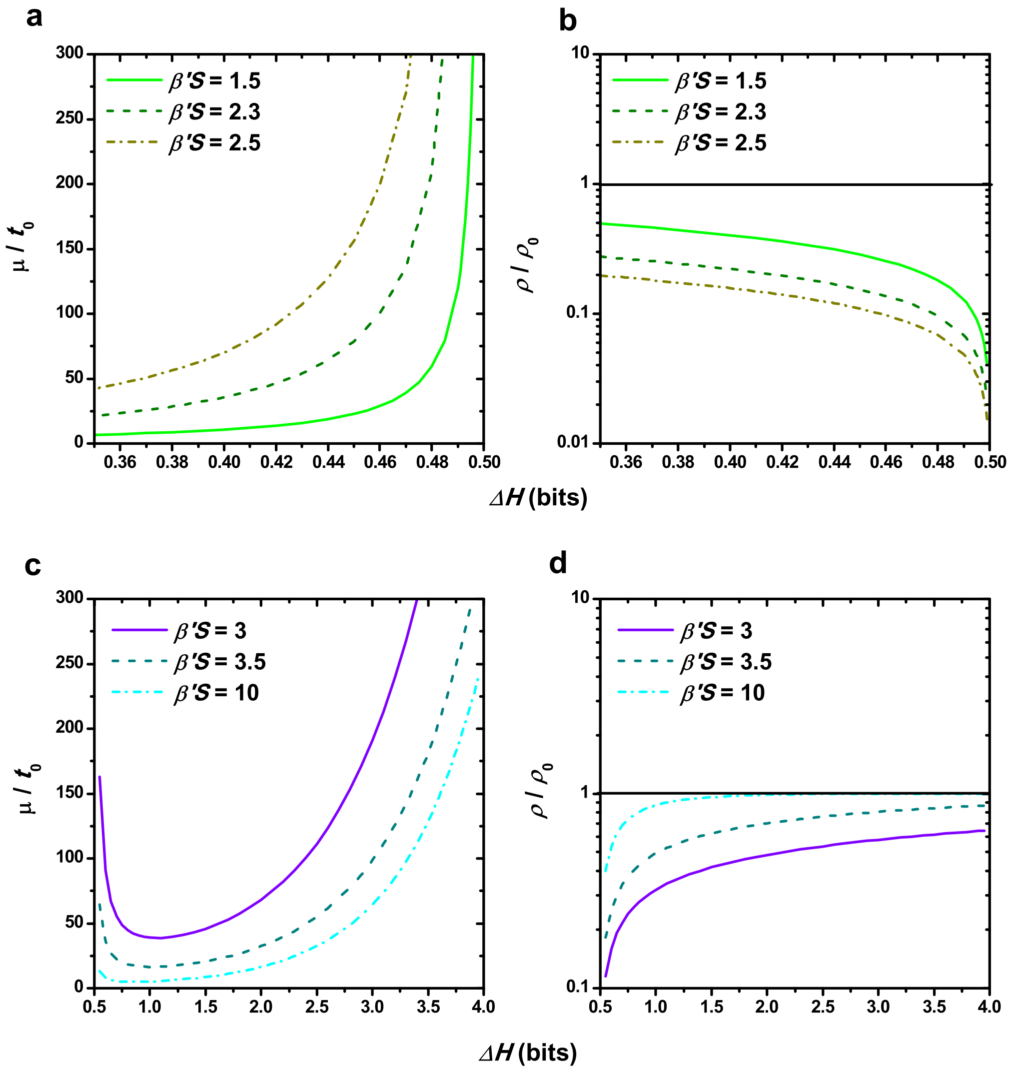

Fig. 4. Panels (a–b) show the linear plot of the normalized mean RT μ/t_0 and the semi-logarithmic plot of the normalized ratio ρ/ρ_0 as a function of the transfer of information for values lower than $\Delta H < 0.5$ bits, respectively. Panels (c–d) are the same as panels (a–b) but for $\Delta H > 0.5$ bits. In all cases, solid, dashed and dash-dotted lines indicate different values of the relative stimulus strength $\beta'S$. In panels (b) and (d) horizontal black solid lines indicate a ratio equal to unity. The normalized sensory threshold has a fixed value of $\ln\left(\beta'S_0\right) = 1$.

Weak additive noise, or equivalently, strong multiplicative noise can be found near the transition, $0.51 \leq \Delta H \leq 1.2$, where the anti-Hick's effect prevails. Low values of $\beta'S < 10$ enhance that weak additive noise effect.

4. Discussion

RTs are a standard tool in human performance such as in skilled chess and soccer players, etc. We have extended previous works and proposed that a signal-dependent multiplicative process with weak additive noise rules Piéron's power-law function and provides a common basis for both Hick's and anti-Hick's effects.

A key point is the time delay produced by the asymptotic term or plateau, μ_0, in Piéron's law. The plateau μ_0 is the irreducible RT, and contains not only those time delays associated to stimulus encoding, but the formation of an internal threshold too, in that chronological order [41]. The dependency of μ_0 with the sensory threshold, $\beta'S_0$, is compatible with those experimental studies that have revealed the existence of a variable threshold mechanism in RTs and Piéron's law [32,33,61,62]. Further, $\beta'S_0$ modulates the effects of the additive over the multiplicative noise at supra-threshold conditions, and explains the differences between simple, and choice RTs (Fig. 2), and between Hick's, and anti-Hick's effects (Fig. 4).

The information-theoretic model of Piéron's law belongs to a class of sigmoidal functions and the reciprocal of Eq. (1) can be written as follows:

$$R = R_{ref}\left[1+\left(\frac{S_0}{S}\right)^p\right]^{-1}, \tag{27}$$

being $R = 1/\mu$, and $R_{ref} = 1/\mu_0$ [32,33,41–45,47]. Sigmoidal functions as Eq. (27) has been used in the aggregation of oxygen to hemoglobin molecules (also called the Hill equation) [63], in enzyme kinetics, and pharmacology (also called the Michaelis–Menten equation) [64,65], in the development of sand seas in granular media [66], etc. In our case, Eq. (27) is formally equivalent to the Naka–Rushton equation in neurophysiology [41,48,65]. This describes a canonical form of gain control of the spike rate in single neurons [67–70]. The RT model links the sigmoidal growth of spikes with the reciprocal of the mean RTs by scale invariance, a form of symmetry usually found in biology and elsewhere [37,48,49].

Our approach to RTs is based on two fundamental features: the existence of a threshold-based mechanism [61,62], and power-law scaling at the threshold [41,44]. The information entropy H-function plays a key role by associating both concepts in Eqs. (4), (7) and (8). Therefore, power-law scaling leads to long-range dependencies and self-affinity, i.e., Piéron's law resembles the Naka–Rushton equation at smaller time scales in a statistical manner [41,48], in the same way as random fractals [37]. In comparison with sequential-sampling models [3,34,35], the information-theoretic model asserts that there is not an accumulation of information at the beginning, and sensory systems are constrained to a maximum uncertainty state giving by Eq. (4). There is a *bona fide* chronological order that is preserved. Here, decision making comes up after efficient stimulus encoding t_0, and evolves irreversibly in time by the formation of the information threshold, $\Delta H \geq 0$ in the RT plateau μ_0. Maximum entropy or uncertainty as modeled by the H-function is compatible with those theories that seek to unify common emergent patterns in nature from distinct generative mechanisms [71–75].

We propose an analogy between the gain of information in RTs, and a phase transition dealing with different states of connectivity between neurons. The entropy change ΔH resembles an *order parameter* by providing a measure of the internal uncertainty in the sensory system, and controlling the entire RT dynamics. The formation of the sensory threshold in Eq. (19) plays the role of a *temperature*-like function; $\Delta H/\Delta H_0 \cong \beta' {S_0}^p$, $\forall \beta' {S_0}^p \ll 1$ (see also Fig. 1(a)). The critical value of $\Delta H = 0.5$ bits separates the growth of the plateau μ_0 into two different regimes at near-threshold conditions (see Fig. 1(b)). That critical value is also responsible of both Hick's and anti-Hick's effects by promoting weak additive noise in Piéron's power-law function at supra-threshold conditions (see Fig. 4).

The scaling exponent, p, describes non-linear effects and different interpretations have been proposed [9,11,40,41, 50,69,76,77]. In Hill-type equations, $p > 1$ often reflects some form of cooperativity between single units [63–65]. Alternatively, p has been derived as the critical exponent of a phase transition in neural networks [78]. In RTs, the higher the scaling exponent, $p \gg 1$, the more abrupt is the increase of the plateau μ_0 at near-threshold conditions (see Fig. 1(b)), and the more abrupt is the hyperbolic decay of Piéron's law at supra-threshold conditions.

Similar results are found at the microscopic level, and the scaling exponent of the Naka–Rushton equation usually spans a wider range of values [69,74,79,80]. It has been argued that marked non-linear effects in this function produces more selective neural responses to external stimuli. Consequently, cortical neurons become biological switches in the sensory pathway [74,80,81]. However, strong non-linear effects represents a limitation at a macroscopic scale, and prevents adaptive sensory-motor control in everyday tasks. Thus, Piéron's law cannot allocate correct responses with accuracy for uncontrolled external stimuli. The sensory-motor system cannot use its own dynamical range, and the RT becomes a bi-stable transition between a maximum value near the threshold and the plateau μ_0, and thus, producing more errors.

Bi-stability in RTs can be circumvented by multiplicative interactions in cascade showing some form of interdependence [50,59]. In our RT framework, each stage is neither complete independent nor a slave of the previous one, but exhibits some form of coordination or self-tuning effects [50]. It is important to note that the information threshold $\Delta H \geq 0$ can be an unstable process in decision making [43–45]. As shown in Figs. 1 and 2, the more complex the task, the higher the transfer of information ΔH and from Eq. (8), the plateau μ_0 of Piéron's law escapes to infinity:

$$\lim_{\Delta H \to \infty} \mu_0 \equiv t_0 \exp(2 \ln 2 \Delta H) \to \infty. \tag{28}$$

The same effect is translated at supra-threshold conditions by the exponential growth of RTs in the Hick's effect [17] (Fig. 3(a)). However, Piéron's law as modeled by a random multiplicative model always drifts to the repulsion barrier or the plateau μ_0 at supra-threshold conditions $\forall S \gg S_0$. Therefore, the sensory system can balance in part those detrimental effects caused by an excess of ΔH mapped into the scaling exponent p. This implies a first form of multiplicative interdependent coordination between stages to minimize errors derived from very large RTs or *misses* at supra-threshold conditions. In general, sensory-motor systems often exhibit a band-limited range due to a trade-off between accuracy and speed [1,3]. This leads to minimize a second type of errors or *false alarms*, defined by those anticipatory responses or fast errors before stimulus presentation [1].

Contrary to a maximization of the information transfer in neurons or an *Infomax* procedure [51,82–86], the random multiplicative model indicates that optimal decision making, and thus, shorter RTs are produced by promoting a minimum in ΔH after efficient stimulus encoding or an *Infomin* procedure [42–44,75]. This implies a second mechanism of interdependent coordination at near-threshold conditions that affects the minimum RT at μ_0, i.e., from Eq. (8) [39,47,58,59], it follows $(\varDelta H \to \infty) \Rightarrow (t_0 \to 0)$, and vice versa. The asymptotic term μ_0 of Piéron's law expands a limited range of values between a minimum and a maximum producing a quasi-stable plateau in most practical situations [47]:

$$\mu_{0_{\mathrm{MIN}}} = t_{0_{\mathrm{MAX}}} \exp(2 \ln 2 \varDelta H_{\mathrm{MIN}}), \tag{29}$$

$$\mu_{0_{\mathrm{MAX}}} = t_{0_{\mathrm{MIN}}} \exp(2 \ln 2 \varDelta H_{\mathrm{MAX}}). \tag{30}$$

Marked non-linear effects with $p \gg 1$ in Piéron's law are rare in most sensory and cognitive tasks. Our results show that the interplay between multiplicative and weak additive noise in Piéron's law favors the enhancement of the hyperbolic decay over a wide range of experimental conditions and promote optimal RTs to be near the encoding time t_0 in the plateau μ_0. This is compatible with theoretical models of neural control operating at the edge of a stability [87,88].

The RT model can be extended to different scenarios. For instance, redundant target effects often lead to shorter RTs when using multiple target detectors within (e.g., binocular summation) and between sensory modalities (e.g., visual–auditory interactions) in a wide variety of conditions [45]. A decrease in the mean RT due to a summation effect from multiple signals is compatible with a lower transfer of information, $\varDelta H \geq 0$, in the same way as in Fig. 2 [42].

In a different approach, the RT model can be applied to examine the functional role of stochastic resonance (SR) in decision making. In its classical form, SR is a counter-intuitive nonlinear phenomenon where the optimal amount of external noise can improve the detection of near-threshold signals. SR in the brain has been demonstrated from single neurons to human behavior with different medical applications [89–92]. This raise a fundamental question about the simultaneous interplay between internal noise, from the sensory system in itself, and the addition of external noise or masking effects [90,93]. Previous works have proposed that differences on SR between human subjects are due in part to their own level of internal noise. Large levels of internal noise may prevent SR [93], and internal noise can also be signal-dependent [94]. In sequential-sampling models of RTs, a SR-like phenomenon can occur by increasing the rate of stochastic accumulation. In vision research, an inverted U-shape function between subjects' performance (e.g., the percentage of correct choices) and the noise level was inferred in random-dot motion tasks [95,96].

Information theoretic measures of SR often exhibit a maximization procedure for different entropy functions (e.g., Shannon, Fisher information, etc.), showing an inverted U-shaped function at intermediate noise levels [89,90]. Our RT model predicts an *Infomin* approach for SR and decision making. We suggest that a possible hallmark of SR in RTs could exhibit an U-shaped function of $\varDelta H$ versus the ratio ρ/ρ_0 of the additive to multiplicative noise strength in Eq. (18). This issue is beyond the scope of the present paper and merits further analysis.

5. Conclusion

Human RTs are a fundamental approach to elucidate the stochastic latency mechanisms in decision making [1,4–6]. Here we have shown that a random multiplicative process with weak additive noise provides a unifying description of Piéron's power-law function in simple and two-choice RTs, and both Hick's and anti-Hick's effects.

In our approach, we have used an information entropy or the H-function that describes the internal uncertainty state of neurons as a function of time [40,53]. This entropy function defines an irreversible process over time, $\varDelta H \geq 0$, and provides a threshold mechanism in RTs by power-law scaling. Optimal decision making is achieved when RTs are shorter by promoting the principle of minimum transfer of information in neurons after efficient stimulus encoding [43,44,47]. The H-function also provides a unified framework to describe many empirical laws of sensory psychophysics [40,54,55].

The methods applied to choice RTs could be extended to investigate random multiplicative processes and decision making in brain disorders such as autism, alzheimer, attention-deficit disorders, etc. The wide applicability of sigmoidal functions in many fields could inspire novel approaches based on multiplicative processes and power-law scaling. For instance, the logistic curve is often used as the squashing function of neural outputs in artificial neural networks and machine learning. The reciprocal of Piéron's law as modeled in Eqs. (7)–(10) could bio-inspire a different strategy by using a limited range of values in the scaling exponent p.

Declaration of competing interest

The authors declare that they have no known competing financial interests or personal relationships that could have appeared to influence the work reported in this paper.

References

[1] R. Luce, Response Times, Oxford University Press, New York, 1986.
[2] J.M. Medina, W. Wong, J.A. Díaz, H. Colonius, Advances in Modern Mental Chronometry, Frontiers Media, Lausanne, 2015.
[3] R. Ratcliff, P.L. Smith, S.D. Brown, G. McKoon, Diffusion decision model: Current issues and history, Trends Cogn. Sci. 20 (4) (2016) 260–281.
[4] D. Laming, Information Theory of Choice-reaction Times, Academic Press, San Diego, CA, 1968.
[5] A.T. Welford, Choice Reaction Time: Basic Concepts, Academic Press, New York, 1980.
[6] D.E. Meyer, A.M. Osman, D.E. Irwin, S. Yantis, Modern mental chronometry, Biol. Psychol. 26 (1–3) (1988) 3–67.
[7] H. Piéron, Recherches sur les lois de variation des temps de latence sensorielle en fonction des intensite's excitatrices, Année Psychol. 20 (1914) 17–96.
[8] H. Piéron, The Sensations, Yale University Press, New Haven, CT, 1952.
[9] J. Baird, Sensation and Judgement, Lawrence Erlbaum Associates, Mahwah, NJ, 1997.

[10] W.P. Banks, Reaction time as a measure of summation of warmth, Percept. Psychophys. 13 (2) (1973) 321–327.

[11] C. Bonnet, M.C. Zamora, F. Buratti, M. Guirao, Group and individual gustatory reaction times and Pieron's law, Physiol. Behav. 66 (4) (1999) 549–558.

[12] P. Overbosch, R. Dewijk, T.J.R. Dejonge, E.P. Koster, Temporal integration and reaction times in human smell, Physiol. Behav. 45 (3) (1989) 615–626.

[13] R. Schweickert, C. Dahn, K. McGuigan, Intensity and number of alternatives in hue identification: Piéron's law and choice reaction time, Percept. Psychophys. 44 (4) (1988) 383–389.

[14] D. Pins, C. Bonnet, On the relation between stimulus intensity and processing time: Piéron's law and choice reaction time, Percept. Psychophys. 58 (3) (1996) 390–400.

[15] P. Wensveen, L.A.E. Huijser, L. Hoek, R.A. Kastelein, Equal latency contours and auditory weighting functions for the harbour porpoise (*Phocoena phocoena*), J. Exp. Biol. 217 (3) (2014) 359–369.

[16] J. Mulsow, C.E. Schlundt, L. Brandt, J.J. Finneran, Equal latency contours for bottlenose dolphins (*Tursiops truncatus*) and California sea lions (*Zalophus californianus*), J. Acoust. Soc. Am. 138 (5) (2015) 2678–2691.

[17] A. Reina, T. Bose, V. Trianni, J.A.R. Marshall, Psychophysical laws and the superorganism, Sci. Rep. 8 (1) (2018) 4387.

[18] M.W. Van der Molen, J.F. Orlebeke, Phasic heart rate change and the U-shaped relationship between choice reaction time and auditory signal intensity, Psychophysiology 17 (5) (1980) 471–481.

[19] P. Jaskowski, D. Wlodarczyk, Task modulation of the effects of brightness on reaction time and response force, Int. J. Psychophysiol. 61 (2) (2006) 98–112.

[20] R.A. Marino, D.P. Munoz, The effects of bottom-up target luminance and top-down spatial target predictability on saccadic reaction times, Exp. Brain Res. 197 (4) (2009) 321–335.

[21] W.E. Hick, On the rate of gain of information, Q. J. Exp. Psychol. 4 (1952) 11–26.

[22] R.W. Proctor, D.W. Schneider, Hick's law for choice reaction time: A review, Q. J. Exp. Psychol. 71 (6) (2018) 1281–1299.

[23] C.P. Shimp, A.L. Froehlich, W.T. Herbranson, Information processing by pigeons (*Columba livia*): Incentive as information, J. Comp. Psychol. 121 (1) (2007) 73–81.

[24] L.E. Longstreth, Hick's law: Its limit is 3 bits, Bull. Psychon. Soc. 26 (1988) 8–10.

[25] K. Kveraga, L. Boucher, H.C. Hughes, Saccades operate in violation of Hick‘s law, Exp. Brain Res. 146 (3) (2002) 307–314.

[26] B.M. Lawrence, A. St. John, R.A. Abrams, L.H. Snyder, An anti-Hick's effect in monkey and human saccade reaction times, J. Vis. 8 (3) (2008) 26–26.

[27] B. Lawrence, An anti-Hick's effect for exogenous, but not endogenous, saccadic eye movements, Exp. Brain. Res. 204 (115) (2010).

[28] B.M. Lawrence, J.S. Weaver, Manipulations of the relationship between response alternatives and exogenous saccade latencies, Exp. Brain Res. 214 (2) (2011) 241.

[29] J.A. Caballero, N.F. Lepora, K.N. Gurney, Probabilistic decision making with spikes: From ISI distributions to behaviour via information gain, PLoS ONE 10 (4) (2015) e0124787.

[30] S. Verdonck, F. Tuerlinckx, The ising decision maker: A binary stochastic network for choice response time, Psychol. Rev. 121 (3) (2014) 422–462.

[31] M. Servant, A. Montagnini, B. Burle, Conflict tasks and the diffusion framework: Insight in model constraints based on psychological laws, Cogn. Psychol. 72 (2014) 162–195.

[32] S. Plainis, I.J. Murray, Neurophysiological interpretation of human visual reaction times: effect of contrast, spatial frequency and luminance, Neuropsychologia 38 (12) (2000) 1555–1564.

[33] I.J. Murray, S. Plainis, Contrast coding and magno/parvo segregation revealed in reaction time studies, Vis. Res. 43 (25) (2003) 2707–2719.

[34] J.D. Schall, Accumulators, neurons, and response time, Trends Neurosci. 42 (12) (2019) 848–860.

[35] P.L. Smith, R. Ratcliff, Psychology and neurobiology of simple decisions, Trends Neurosci. 27 (3) (2004) 161–168.

[36] H.F. Stanley, P. Meakin, Multifractal phenomena in physics and chemistry, Nature 335 (6189) (1988) 405–409.

[37] M. Schroeder, Fractals, Chaos, Power Laws: Minutes from an Infinite Paradise, W. H. Freeman, New York, 1991.

[38] M.E.J. Newman, Power laws, Pareto distributions and Zipf's law, Contemp. Phys. 46 (5) (2005) 323–351.

[39] D. Sornette, Critical Phenomena in Natural Sciences, Springer-Verlag, Berlin, Heidelberg, 2004.

[40] K.H. Norwich, Information, Sensation, and Perception, Academic Press, San Diego, CA, 1993.

[41] J.M. Medina, 1/f(alpha) noise in reaction times: A proposed model based on Pieron's law and information processing, Phys. Rev. E 79 (1) (2009).

[42] J.M. Medina, Effects of multiplicative power law neural noise in visual information processing, Neural Comput. 23 (4) (2011) 1015–1046.

[43] J.M. Medina, Multiplicative processes and power laws in human reaction times derived from hyperbolic functions, Phys. Lett. A 376 (19) (2012) 1617–1623.

[44] J.M. Medina, J.A. Díaz, K.H. Norwich, A theory of power laws in human reaction times: insights from an information-processing approach, Front. Hum. Neurosci. 8 (621) (2014) 1–4.

[45] J.M. Medina, J.A. Díaz, Commentary: Piéron's law is not just an artifact of the response mechanism, Front. Physiol. 6 (190) (2015) 1–4.

[46] J.M. Medina, J.A. Díaz, Extreme reaction times determine fluctuation scaling in human color vision, Physica A 461 (2016) 125–132.

[47] J.M. Medina, J.A. Díaz, Noise-induced transition in human reaction times, J. Stat. Mech. Theory Exp. 2016 (9) (2016) 093502.

[48] N. Chater, G.D.A. Brown, Scale-invariance as a unifying psychological principle, Cognition 69 (3) (1999) B17–B24.

[49] T. Gisiger, Scale invariance in biology: coincidence or footprint of a universal mechanism? Biol. Rev. 76 (2) (2001) 161–209.

[50] C.T. Kello, G.D.A. Brown, R. Ferrer-i Cancho, J.G. Holden, K. Linkenkaer-Hansen, T. Rhodes, G.C. Van Orden, Scaling laws in cognitive sciences, Trends Cogn. Sci. 14 (5) (2010) 223–232.

[51] J.M. Beggs, The criticality hypothesis: how local cortical networks might optimize information processing, Phil. Trans. R. Soc. A 366 (1864) (2008) 329–343.

[52] H.O. Peitgen, H. Jürgens, D. Saupe, Chaos and Fractals, Springer-Verlag, New York, 1992.

[53] K.H. Norwich, C.N.L. Seburn, E. Axelrad, An informational approach to reaction times, Bull. Math. Biol. 51 (3) (1989) 347–358.

[54] K.H. Norwich, W. Wong, A universal model of single-unit sensory receptor action, Math. Biosci. 125 (1) (1995) 83–108.

[55] K.H. Norwich, W. Wong, Unification of psychophysical phenomena: The complete form of Fechner's law, Percept. Psychophys. 59 (6) (1997) 929–940.

[56] H. Takayasu, A.H. Sato, M. Takayasu, Stable infinite variance fluctuations in randomly amplified langevin systems, Phys. Rev. Lett. 79 (6) (1997) 966–969.

[57] H. Nakao, Asymptotic power law of moments in a random multiplicative process with weak additive noise, Phys. Rev. E 58 (2) (1998) 1591–1600, PRE.

[58] D. Sornette, R. Cont, Convergent multiplicative processes repelled from zero: Power laws and truncated power laws, J. Phys. 7 (3) (1997) 431–444.

[59] D. Sornette, Multiplicative processes and power laws, Phys. Rev. E 57 (4) (1998) 4811–4813.

[60] Z. Eisler, I. Bartos, J. Kertész, Fluctuation scaling in complex systems: Taylor's law and beyond, Adv. Phys. 57 (1) (2008) 89–142.

[61] P. Heil, H. Neubauer, A. Tiefenau, H. von Specht, Comparison of absolute thresholds derived from an adaptive forced-choice procedure and from reaction probabilities and reaction times in a simple reaction time paradigm, J. Assoc. Res. Otolaryngol. 7 (3) (2006) 279.
[62] C.-C. Lo, X.-J. Wang, Cortico-basal ganglia circuit mechanism for a decision threshold in reaction time tasks, Nat. Neurosci. 9 (7) (2006) 956–963.
[63] A.V. Hill, The possible effects of the aggregation of the molecules of haemoglobin on its dissociation curves, J. Physiol. 40 (suppl) (1910) i–vii.
[64] L. Michaelis, M.L. Menten, Die kinetik der invertinwirkung, Biochem. Z. 49 (1913) 333–369.
[65] J.D. Murray, Mathematical Biology, third ed., Springer-Verlag, Berlin, Germany, 2002.
[66] T. Shinbrot, T. Sabuwala, T. Siu, L.M. Vivar, P. Chakraborty, Size sorting on the rubble-pile asteroid Itokawa, Phys. Rev. Lett. 118 (11) (2017) 111101.
[67] K.I. Naka, W.A.H. Rushton, S-potentials from luminosity units in retina of fish (cyprinidae), J. Physiol. London 185 (3) (1966) 587–599.
[68] V. Torre, J.F. Ashmore, T.D. Lamb, A. Menini, Transduction and adaptation in sensory receptor cells, J. Neurosci. 15 (12) (1995) 7757–7768.
[69] V.A. Billock, B.H. Tsou, To honor fechner and obey stevens: Relationships between psychophysical and neural nonlinearities, Psychol. Bull. 137 (1) (2011) 1–18.
[70] M. Carandini, D.J. Heeger, Normalization as a canonical neural computation, Nat. Rev. Neurosci. 13 (1) (2012) 51–62.
[71] E.T. Jaynes, Information theory and statistical mechanics, Phys. Rev. 106 (4) (1957) 620–630.
[72] H. Haken, Information and Self-Organization, third ed., Springer-Verlag, Berlin, 2006.
[73] L.M. Martyushev, V.D. Seleznev, Maximum entropy production principle in physics, chemistry and biology, Phys. Rep. 426 (1) (2006) 1–45.
[74] S.A. Frank, Input-output relations in biological systems: measurement, information and the Hill equation, Biol. Direct 8 (1) (2013) 31.
[75] V.I. Yukalov, D. Sornette, Self-organization in complex systems as decision making, Adv. Complex Syst. 17 (03n04) (2014) 1450016.
[76] M. Copelli, A.C. Roque, R.F. Oliveira, O. Kinouchi, Physics of psychophysics: Stevens and Weber-Fechner laws are transfer functions of excitable media, Phys. Rev. E 65 (6) (2002) 060901(R).
[77] D.M. Mackay, Psychophysics of perceived intensity: a theoretical basis for Fechners ans Stevens laws, Science 139 (356) (1963) 1213–1216.
[78] O. Kinouchi, M. Copelli, Optimal dynamical range of excitable networks at criticality, Nat. Phys. 2 (5) (2006) 348–352.
[79] D.G. Albrecht, D.B. Hamilton, Striate cortex of monkey and cat: contrast response function, J. Neurophysiol. 48 (1) (1982) 217–237.
[80] G. Sclar, J.H.R. Maunsell, P. Lennie, Coding of image-contrast in central visual pathways of the macaque monkey, Vis. Res. 30 (1) (1990) 1–10.
[81] W.S. Geisler, D. Albrecht, Bayesian analysis of identification performance in monkey visual cortex: nonlinear mechanisms and stimulus certainty, Vis. Res. 35 (19) (1995) 2723–2730.
[82] S. Laughlin, A simple coding procedure enhances a neuron's information capacity, Z. Nat.forsch. C 36 (9–10) (1981) 910–912.
[83] R. Linsker, Self-organization in a perceptual network, Computer 21 (3) (1988) 105–117.
[84] R. Linsker, Perceptual neural organization: some approaches based on network models and information theory, Ann. Rev. Neurosci. 13 (1990) 257–281.
[85] A. Gottschalk, Derivation of the visual contrast response function by maximizing information rate, Neural Comput. 14 (3) (2002) 527–542.
[86] J.M. Beggs, D. Plenz, Neuronal avalanches in neocortical circuits, J. Neurosci. 23 (35) (2003) 11167–11177.
[87] M. Venkadesan, J. Guckenheimer, F.J. Valero-Cuevas, Manipulating the edge of instability, J. Biomech. 40 (8) (2007) 1653–1661.
[88] J.G. Milton, The delayed and noisy nervous system: implications for neural control, J. Neural Eng. 8 (6) (2011) 065005.
[89] L. Gammaitoni, P. Hanggi, P. Jung, F. Marchesoni, Stochastic resonance, Rev. Modern Phys. 70 (1) (1998) 223–287.
[90] F. Moss, L.M. Ward, W.G. Sannita, Stochastic resonance and sensory information processing: a tutorial and review of application, Clin. Neurophysiol. 115 (2) (2004) 267–281.
[91] A.A. Faisal, L.P.J. Selen, D.M. Wolpert, Noise in the nervous system, Nat. Rev. Neurosci. 9 (4) (2008) 292–303.
[92] M.D. McDonnell, L.M. Ward, The benefits of noise in neural systems: bridging theory and experiment, Nat. Rev. Neurosci. 12 (7) (2011) 415–U89.
[93] T. Aihara, K. Kitajo, D. Nozaki, Y. Yamamoto, How does stochastic resonance work within the human brain? — Psychophysics of internal and external noise, Chem. Phys. 375 (2–3) (2010) 616–624.
[94] G.A. Cecchi, M. Sigman, J.M. Alonso, L. Martinez, D.R. Chialvo, M.O. Magnasco, Noise in neurons is message dependent, Proc. Natl. Acad. Sci. 97 (10) (2000) 5557–5561.
[95] M. Treviño, B. De la Torre-Valdovinos, E. Manjarrez, Noise improves visual motion discrimination via a stochastic resonance-like phenomenon, Front. Hum. Neurosci. 10 (572) (2016).
[96] O. van der Groen, M. Tang, N. Wenderoth, J. Mattingley, Stochastic resonance enhances the rate of evidence accumulation during combined brain stimulation and perceptual decision-making, PLoS Comput. Biol. 14 (7) (2018) e1006301.